JOURNAL OF GEOPHYSICAL RESEARCH, VOL. 101, NO. D14, PAGES 19,109-19,118, AUGUST 27, 1996

Interannual variations in Antarctic precipitation related to El Niño-Southern Oscillation

Richard I. Cullather and David H. Bromwich

Polar Meteorology Group, Byrd Polar Research Center, Ohio State University, Columbus

Michael L. Van Woert

Office of Naval Research, Arlington, Virginia

Abstract. The accurate estimation of Antarctic precipitation variability is an essential component in understanding global sea level fluctuations; direct measurement techniques, however, are replete with practical difficulties. In this study, net precipitation (precipitation minus sublimation) for the Antarctic continent is computed for 1980-1994 using operational numerical analyses obtained from the ECMWF (European Centre for Medium-Range Weather Forecasts). The resulting estimations reveal a strong interannual variability for the Antarctic continent, implying a ±1.2 - 1.5 mm yr^{-1} maximum range in the Antarctic eustatic change contribution. In particular, variability for the South Pacific sector (120°W-180°W) is shown to be correlated with the El Niño-Southern Oscillation (ENSO) phenomenon for 1980-1990. The relation becomes anticorrelated after 1990, associated with a strong East Antarctic ridging pattern that coincides with the start of the prolonged series of warm events of the early 1990s. This result is relevant to other studies relating ENSO variability to high southern latitudes, and a more elaborate picture of this teleconnection pattern is presented. Comparisons of sea level pressure values using available ship observations show good agreement and offer a confirmation of the analyses in this data-sparse region. Additionally, a comparison of results with values obtained from the precipitation fields of the NCEP/NCAR (NCEP: National Centers for Environmental Prediction; NCAR: National Center for Atmospheric Research) reanalysis project are discussed.

1. Introduction

Analyzed grids of observed and derived variables produced by operational weather centers have been applied with increasing regularity to a variety of atmospheric topics. These analyzed grids are the results of the four-dimensional assimilation of meteorological observations and are used to initialize global forecast models. They represent the integration of all available sources of atmospheric information, including satellite data [*Trenberth*, 1992]. Recent studies have demonstrated the feasibility of computing net precipitation (precipitation minus sublimation) for the Antarctic continent from a variety of numerical analyses using the atmospheric moisture budget approach [*Yamazaki*, 1992; *Budd et al.*, 1995; *Bromwich et al.*, 1995]. This approach is particularly useful in providing reliable net precipitation estimates, owing to the limitations and complexities involved in direct measurement techniques [*Bromwich*, 1988]. Previously, no record of Antarctic precipitation temporal variability has been available for scales ranging from regional to continental, despite the dominant importance of precipitation for ice sheet mass balance and consequential relevance to global sea level variability [*Oerlemans*, 1989; *Jacobs*, 1992].

Using the record provided by the analyses, the interannual variations in the net precipitation record are examined here. Specifically, the impact of the El Niño-Southern Oscillation (ENSO) phenomenon on the atmospheric hydrologic cycle in Antarctica is investigated. Perhaps the most widely recognized source of climatic variation, ENSO is principally centered in the tropical and subtropical latitudes of the South Pacific Ocean with global teleconnections [*Trenberth*, 1991a]. Studies relating ENSO to high southern latitudes have increased recently, despite the relatively short record of conventional Antarctic meteorological data. An initial literature review was made by *Bromwich et al.* [1991]. Variations in sea level pressure (SLP) and height field anomalies for the southern hemisphere, including Antarctica and vicinity, have been examined by *van Loon and Shea* [1987] and *Karoly* [1989] using analyzed fields. *Smith and Stearns* [1993a b] expanded on earlier work by *Savage et al.* [1988] in correlating Antarctic surface pressure and temperature anomalies to ENSO using values obtained from manned stations. Particularly numerous are studies indicating a teleconnection with variations in Antarctic sea ice extent [*Chiu*, 1983; *Carleton*, 1988, 1989; *Xie et al.*, 1994; *Simmonds and Jacka*, 1995; *Gloersen*, 1995]. Xie et al. refer to this relation between ENSO events and Antarctic sea ice as the Southern Oceanic Oscillation (SOO).

As the number of observational studies continues to grow, identification of the mechanisms involved in propagation of the ENSO signal has evolved considerably. *Newell et al.* [1981] (reviewed by *Pittock* [1984]) first speculated that possible high-latitude forcing of the Southern Oscillation could be achieved by atmospheric forcing of the Antarctic Circumpolar Current and subsequent SST (sea surface

Paper number 96JD01769.
0148-0227/96/96JD-01769$09.00

temperature) propagation northward via the Peru Current. More recent articles, however, have focused on the role of the South Pacific atmospheric double jet variability in the southward propagation of the ENSO signal [*Kitoh*, 1994; *Smith and Bromwich*, 1994; *Smith et al.*, 1995; *Chen et al.*, 1996]. Tracks of cyclones and anticyclones in this region have been found to be strongly influenced by the double jet [*Sinclair*, 1996]. The variability of the double jet is illustrated in Figure 1 [after *Chen et al.*, 1996] using the European Centre for Medium-Range Weather Forecasts (ECMWF) analyses in comparison with the Southern Oscillation Index (SOI), defined here as the standard Tahiti minus Darwin sea level pressure anomaly, obtained from the U.S. National Centers for Environmental Prediction (NCEP, formerly National Meteorological Center (NMC)) Climate Prediction Center (CPC). As observed by *Chen et al.* [1996], the subtropical jet around 30°S strengthens during ENSO warm phases (SOI < 0), while the polar front jet near 60°S strengthens during cold or normal phases (SOI ≥ 0). The polar front jet behavior is more variable and less well defined than that of the subtropical jet. The nature and role of the double jet oscillation is not well understood, however, and further observational study of the ENSO–high southern latitude relation is necessary if a complete understanding of the teleconnection is to be realized. Increasingly, this teleconnection pattern is being invoked in research areas outside of those associated with atmospheric and physical oceanographic phenomena, for example, to explain variations in the abundance of Southern Ocean marine life [*Priddle et al.*, 1988; *Dayton*, 1989; *Testa et al.*, 1991].

2. Data and Calculations

In this study, moisture fluxes are computed using the ECMWF WMO (World Meteorological Organization) initialized archive from 1980-1989, and the uninitialized ECMWF WCRP/TOGA (Tropical Oceans Global Atmosphere, a program under the World Climate Research Program) Archive II for 1985-1994 obtained from the National Center for Atmospheric Research (NCAR). Both ECMWF analyses are produced twice daily (0000 and 1200 UTC) and are archived on a 2.5° latitude/longitude grid.

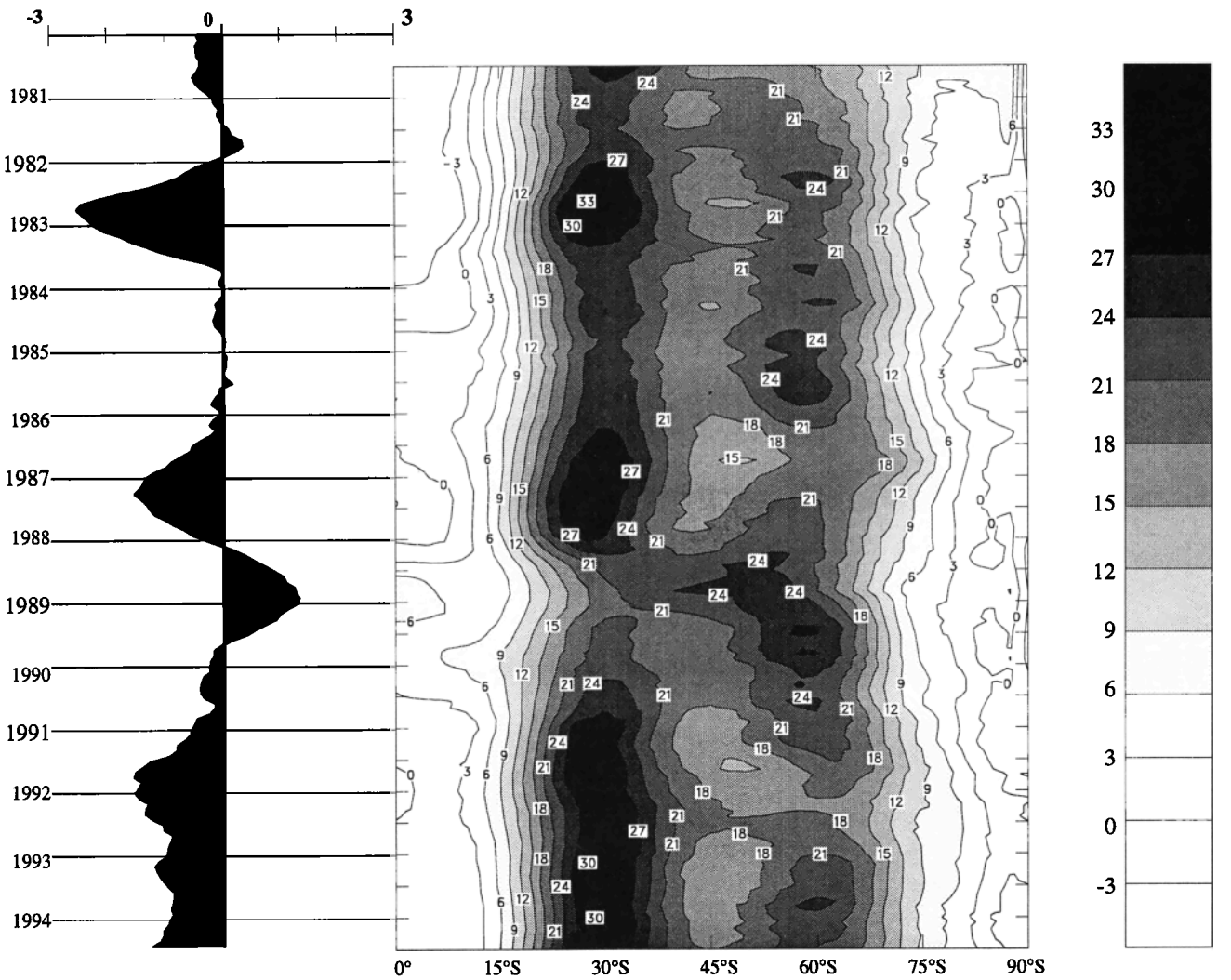

Figure 1. Hovmöller diagram of annual running mean 300-hPa zonal wind averaged over 120°W-180°W from ECMWF WMO (1980-1989) and WCRP/TOGA II (1985-1994) archives, in meters per second. For overlapping years, the two archives are averaged. On the left is the annual running mean NCEP Climate Prediction Center Southern Oscillation Index (SOI) in hectopascals.

Wind fields from the WCRP/TOGA archive are available at 10 m and 14 standard pressure levels to 10 hPa. The WMO archive contains data at seven standard pressure levels to 100 hPa. Moisture values in both analyses are available up to the 300-hPa level.

A major obstacle to using analyzed data for climatic studies is the effect of alterations in the data assimilation system on the climatic ensemble of analyses [*Trenberth*, 1992]. Additionally, inconsistencies in the Antarctic analyses are known to exist for the early period through 1982 [*Trenberth*, 1992]. Nevertheless, the analyzed grids represent the most comprehensive assimilation of satellite and conventional meteorological data available. *Trenberth and Guillemot* [1995] have evaluated the ECMWF atmospheric moisture budget from a global perspective. Substantial differences with other analyses, as well as artificial trends, are found, particularly in the tropics, where the effect of the model cumulus parameterization can be significant, and in the subtropics as a results of the assimilation of biased TOVS (TIROS operational vertical sounder) retrievals. In the southern hemisphere, *Bromwich et al.* [1995] have evaluated the derived atmospheric moisture budget against rawinsonde and glaciological observations. A comparison of analyses obtained from the ECMWF, the NMC, and the Australian Bureau of Meteorology indicated that the analyses produced by the ECMWF more closely reproduce time-averaged Antarctic glaciological data and rawinsonde values at each level and were generally found to provide reliable precipitation estimates for the Antarctic. *Genthon and Braun* [1995] have examined ECMWF model precipitation fields over Antarctica from ensemble accumulation predictions for 1985-1991 and have found good agreement with available observations. Results of *Genthon and Braun* [1995] indicate that the ECMWF depiction does a fairly good job with atmosphere-surface water exchange over ice sheets. Genthon and Braun also describe deficiencies in the topographic treatment used by ECMWF. The use of the "envelope" topographic representation by ECMWF creates significant inaccuracies in the vicinity of high elevation gradients. In Antarctica, however, the largest topographic errors occur over Queen Maud Land (30°W-60°E) [*Genthon and Braun*, 1995, see their Figure 3].

Aside from the moisture budget, two other studies of the analyses skill are worth noting. *Arpe and Cattle* [1993] evaluated wind stresses derived from the analyses of the ECMWF and the United Kingdom Meteorological Office for 1988-1990. The two analyses were found to be similar over the Antarctic sea ice zone in general, although large discrepancies arose from the acceptance of an individual observation in one analysis and the rejection in another. *Escoffier and Provost* [1995] compared observed wind forcing over the southwest Atlantic with the ECMWF analyses for 1986-1990. The largest discrepancies were found to be due to localized land-sea effects not resolved by the analyses, and agreement with observed annual and semiannual signals was found to be exceptional. Although some significant discrepancies with observations are noted, these studies imply a preference for the ECMWF analyses for atmospheric study of the southern hemisphere. The ECMWF analyses currently represent the most comprehensive assimilation of satellite and conventional meteorological data available.

The atmospheric moisture budget may be expressed as

$$\frac{\partial \overline{W}}{\partial t} + \nabla \cdot \frac{1}{g} \int_0^{P_{sfc}} \overline{qV^*}\, dp = \overline{E} - \overline{P} \tag{1}$$

where W is precipitable water, g is gravity, q is specific humidity, V^* is the horizontal wind field corrected for violations of the conservation of mass, P_{sfc} is surface pressure, E is rate of evaporation/sublimation per unit mass, and P is precipitation rate. An overbar indicates a time average. From both the analyses and observations [*Bromwich*, 1988], the first term on the left, referred to as the storage term, is found to be small over interannual timescales. The remainder may be rewritten as [e.g., *Bromwich and Robasky*, 1993]

$$\left\langle \overline{P} - \overline{E} \right\rangle = -\frac{1}{A} \oint \left\{ \int_0^{P_{sfc}} \frac{\overline{qV^*}}{g} dp \right\} \cdot \boldsymbol{n}\, dl \tag{2}$$

where A is the area over which the net precipitation is to be determined, and $\boldsymbol{n}$ is the outward normal to the area perimeter. The angled brackets indicate an areal average. Monthly mean and eddy components have also been computed using

$$\overline{qV} = \overline{q}\,\overline{V} + \overline{q'V'} \tag{3}$$

where prime denotes an eddy value. The second term on the right-hand side may be written

$$\overline{q'V'} = \overline{(q - \overline{q})(V - \overline{V})} \tag{4}$$

In practice, corrections to the moisture transports for mass balance can be made only at each time step and hence are computationally expensive. These corrections have not been included in results presented here. *Bromwich et al.* [1995] presented results for the Antarctic moisture budget on a continental scale. At the grid box scale, however, the moisture convergence field becomes excessively noisy and is subject to large variations in the mass balance error. This is particularly true in high southern latitudes, where the longitudinal grid spacing approaches zero and steep topography is present. Horizontal resolution has been shown not to be a big factor on large scales, however, even for locations where steep gradients exist in precipitation [*Trenberth and Guillemot*, 1995]; the sector and continental areas described below and shown in Figure 2 are 1.4 million and 13 million km^2, respectively. *Trenberth* [1991b] outlined a strategy for correcting mass imbalance using the ECMWF analyses in spectral format. This strategy has been applied to gridded analyses for the southern hemisphere for selected months of 1994 to assess the impact on the moisture budget, using computational procedures given by *Swarztrauber* [1974]. At an individual box, the applied correction can be substantial; for the regions given in Figure 2, however, the correction is of the order of a few millimeters per year for the months computed and is thus ignored.

3. Results

Evaluation of West Antarctic Moisture Convergence

In Figure 2 the Antarctic continent and a selected South Pacific sector are shown. The region chosen is in West Antarctica and directly south of the South Pacific double jet

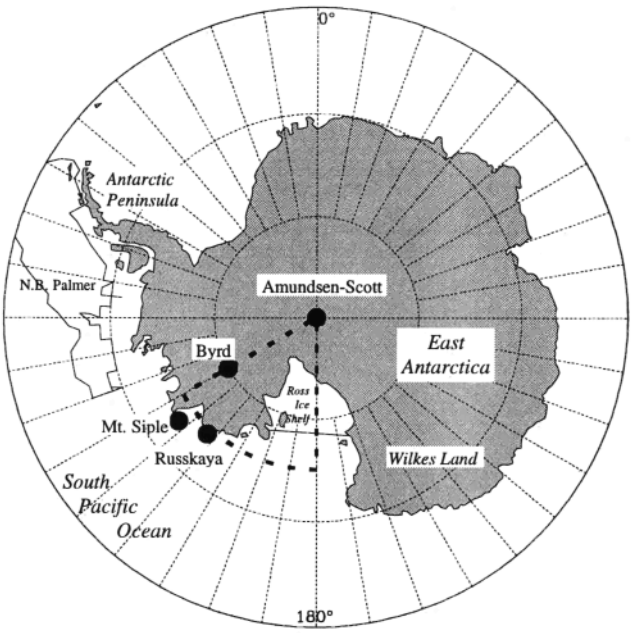

Figure 2. Antarctic continent, with outline of South Pacific moisture convergence sector (dashed lines), significant West Antarctic stations, and the track of the ship *Nathaniel B. Palmer*. Grid lines are shown for every 10° latitude/longitude.

domain, with longitudinal boundaries corresponding to those used in producing Figure 1. Previous studies of Antarctic precipitation have indicated that disproportionately large moisture fluxes occur in West Antarctica [*Lettau*, 1969], where cyclonic activity is able to penetrate inland. South Pacific cyclonic activity has been found to be influenced by the oscillatory strengthening and weakening of the subtropical and polar front jets associated with ENSO [*Karoly*, 1989; *Smith et al.*, 1995; *Sinclair*, 1996; *Chen et al.*, 1996]. From the ECMWF analyzed grids, nearly 40% of the moisture transport into Antarctica occurs along the West Antarctic coast. The South Pacific sector shown in Figure 2 marshals available data from the sparse West Antarctic surface network. The western border is anchored by an array of automatic weather stations [*Stearns et al.*, 1993] on the Ross Ice Shelf. The northern border is chosen to approximate the West Antarctic coastline, and is bounded to the east by Russkaya station, available during the analysis period until March 1990, and the automatic weather station at Mount Siple, operational since February 1992.

Figure 3 presents the computed interannual trend in moisture convergence for Antarctica and the West Antarctic sector, with the latter compared with the SOI. During the time period investigated, the ENSO cycle experiences one well-defined cold event (SOI > 0) in 1988-1989 and three warm events (SOI < 0) in 1982, 1987, and an extended period beginning in 1991, with the 1982 event being the strongest this century [*National Research Council*, 1983]. For validation purposes, the Antarctic continent is defined similarly to *Giovinetto and Bentley* [1985] to include the major ice shelves and exclude the Antarctic Peninsula region north of 70°S. Moisture convergence for the Antarctic continent prior to 1990 generally reflects the ENSO trend, with smaller values during warm events and larger values during normal or cold events. Reasonable agreement exists between the WMO and WCRP/TOGA archive trends during overlapping years (1985-1989). The ECMWF long-term average is 149 mm yr^{-1}, with an annual standard deviation of 24 mm yr^{-1}, and compares well with the long-term glaciological value of 151-156 ±15 mm yr^{-1} [*Bromwich*, 1990].

The lower portion of Figure 3 shows the predominant influence of the ENSO signal in the South Pacific sector. Agreement prior to 1990 is very striking, given the broad range experienced by the SOI. Moisture convergence decreases during warm events and increases during cold events with nearly the same phase and amplitude of the SOI. Again, inconsistencies in the Antarctic analyses are known to exist for the early period through 1982. From 1982 until 1989, the correlation coefficient between the SOI and the

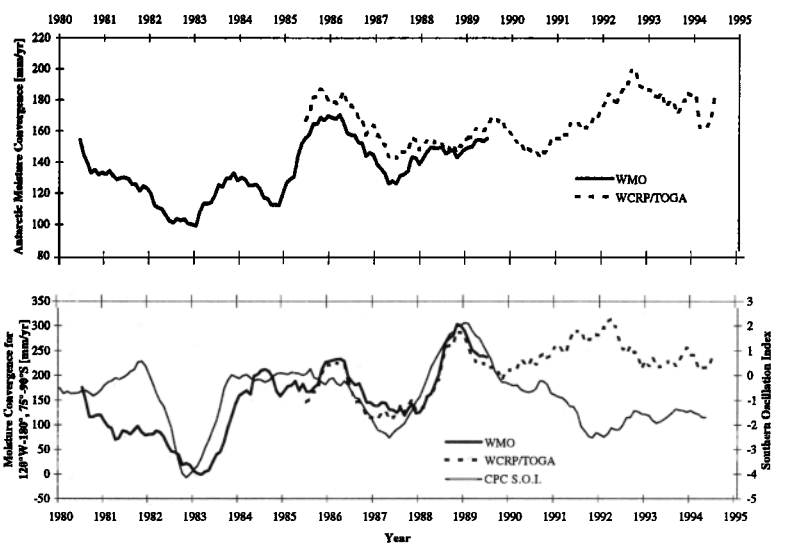

Figure 3. Twelve-month centered running-mean moisture convergence (in millimeters per year) for Antarctica (top) and West Antarctic sector (bottom) in comparison with the Southern Oscillation Index (in hectopascals).

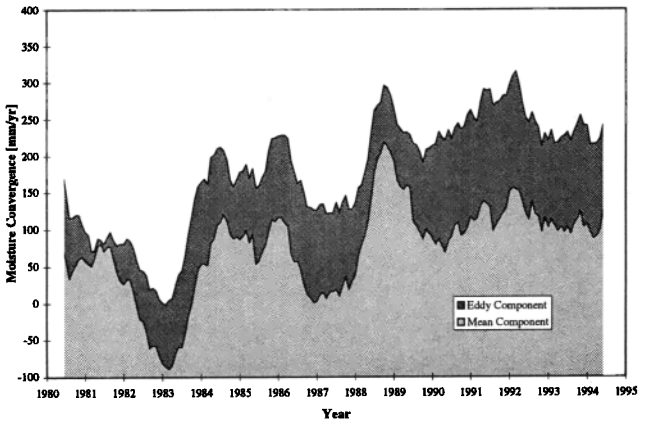

Figure 4. As in the lower part of Figure 3, but showing the contribution of mean and eddy components of the West Antarctic moisture convergence (in millimeters per year). For overlapping years, the two archives are averaged.

WMO archive is 0.87. From 1985 until 1990, the correlation coefficient with the WCRP/TOGA archive is 0.88. The long-term average is 183 mm yr^{-1}, with a standard deviation of 77 mm yr^{-1}, and is within the range from long-term glaciological data [*Giovinetto and Bentley*, 1985; *Giovinetto et al.*, 1992] of 144±14 mm yr^{-1}. The range shown is dramatic. Essentially, zero annual net precipitation is estimated during the 1982-1983 SOI minimum, and more than 300 mm yr^{-1} is estimated for the 1988-1989 SOI maximum. The sector plot in Figure 3 is subdivided into mean and eddy components in Figure 4. Eddy transport generally dominates in high southern latitudes; in West Antarctica, however, the mean and eddy components are of the same order, again consistent with Lettau [1969]. In Figure 4, the mean component accounts for an average of 42% of the moisture convergence. Almost all of the ENSO-related interannual variability is found to occur in the mean component.

Amundsen Sea Low

Figure 5 shows the pattern of moisture flux vectors prior to (left) and during (right) West Antarctic interannual low precipitation events, here represented by the 1982 event. The depicted mean sea level pressure field resolves the Amundsen Sea Low, a climatological feature associated with cyclonic activity propagating into the region. Under normal net precipitation conditions (left), the annually averaged low occupies a position near the eastern Ross Ice Shelf. Moisture is transported directly into the sector from almost due north. When low net precipitation is recorded (right), the low occupies a location significantly farther east and closer to the Antarctic Peninsula. The moisture transport that previously reached the West Antarctic sector is now deflected toward the peninsula region. A portion of this transport wraps around the low and enters the sector across the eastern boundary. This is more clearly realized in Figure 6, which shows the contributions to sector moisture convergence from the individual boundaries. The contributions from the eastern and northern boundaries are out of phase, consistent with the positioning of the low. The eastern component is generally less than the contribution from the north. Only during the ENSO warm events of 1982-1983 and 1987 is the eastern component larger. The distance between the locations of the low during normal and reduced precipitation is typically 1400 km. This relation between net precipitation and Amundsen Sea Low positioning remains consistent for the 15-year period examined.

It should be clear that if the sector had been selected closer to the peninsula region, the interannual net precipitation variability would become out of phase with the original sector. In actuality, a lead or lag in the correlation of net precipitation with the original sector is dependent on the longitudinal positioning and orientation with respect to the Amundsen Sea Low. The phase relationship seen here has also previously been noted as an anticorrelation in sea ice extent between the Bellingshausen and Ross Seas [*Harangozo*, 1995].

East Antarctic Ridging

Equally as striking as the correlation between the West Antarctic moisture convergence and SOI prior to 1990 is the anticorrelation after 1990 (Figure 3), coinciding with an extended ENSO event [*Trenberth and Hoar*, 1996]. The

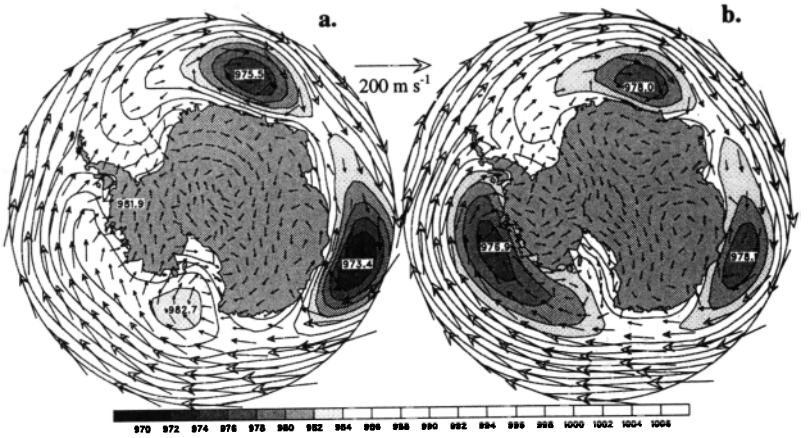

Figure 5. Typical annual mean pressure patterns for (a) normal (1980) and (b) reduced (1982) West Antarctic precipitation events. Vectors represent vertically integrated moisture flux (plotted maximum vector is 200 kg m^{-1} s^{-1}). Mean sea level pressure field is contoured every 2 hPa.

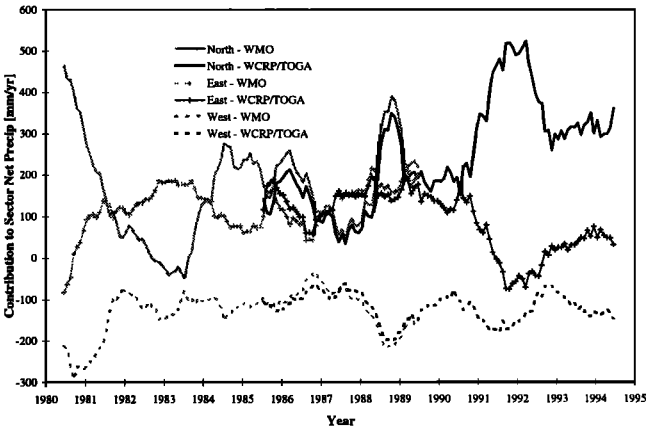

Figure 6. Twelve-month centered running-means of vertically integrated moisture transports across boundaries of the West Antarctic sector, in millimeters per year.

South Pacific sector and the Antarctic continent show a marked increase in moisture convergence beginning in 1990, nearly mirroring the decrease in the SOI. Two aphysical reasons are considered: substantial changes to the analysis assimilation physics in May 1989 and the closing of Russkaya station in March 1990.

It is doubtful that changes to the analysis scheme would so adversely affect the trend. Large increases in moisture convergence for the Antarctic continent were also found in NMC and Australian Bureau of Meteorology analyses for 1990-1992 [*Bromwich et al.*, 1995]. While the closing of Russkaya must have detracted from the analyses, the oscillatory changes depicted in Figure 5 appear be of a scale large enough to be resolved by observations from station arrays on the Ross Ice Shelf and the peninsula. Moreover, the addition of the Mount Siple automatic weather station in early 1992 does not affect the anticorrelated trend. A comparison of the ECMWF mean sea level pressure with values obtained by the R/V *Nathaniel B. Palmer* research vessel for August and September 1993 [*Jefferies*, 1994] (acquired from University of Wisconsin-Madison), shown in Figure 7, confirms the accuracy of the analysis in the absence of the Russkaya station but with the Mount Siple automatic weather station operating. Analyses values shown were interpolated from the nearest grid boxes. Values contaminated by nearby mountainous terrain on the peninsula were removed from the ECMWF time series. The ship observations plotted were not available to ECMWF via the Global Telecommunications System (GTS) (British Antarctic Survey, personal communication). The correlation coefficient is greater than 0.94, with a standard error for ECMWF values of less than 5 hPa from each ship observation in the regression, indicating consistent agreement. The close correlation is excellent, considering the large variability in observed values. Observations varied from 1014 hPa to a low reading of 934.3 hPa. The analyzed value for the latter report was 10 hPa higher. The comparison is particularly surprising, given the ship is translating through the gridded field.

It may then be concluded that the observed change is due to real changes in the atmospheric circulation. This change is discernible from annually averaged 500-hPa geopotential height fields shown in Figure 8. At the time of the change in the association shown in Figure 3, a ridge pattern begins to dominate the Wilkes Land region of East Antarctica and continues through 1994. The anticyclonic pattern is in close proximity to the low and appears to interact in a quasi-omega blocking pattern [e.g., *Bluestein*, 1993]. A ridging feature in East Antarctica is present in 1982-1984, but this event is not as marked and is farther from the low, near 100°E. In contrast, the Wilkes Land ridging pattern in 1991-1994 is clearly more pronounced. A seasonal analysis indicates this feature occurs year-round. The ridging can be easily identified in the mean moisture transport pattern shown in Figure 9. In 1986, a weak anticyclonic pattern is present in Wilkes Land but is completely dominated by the main vortex over the Ross Ice Shelf and a second low near Mawson station. The 1986 pattern is typical of most years in the 1980s. In 1988, a larger ridging feature first becomes apparent. The cyclonic feature over the ice shelf still dominates the mean flow, however. In 1990, the ridge displays a closed-off circulation pattern. The streamline pattern for 1992, however, is significantly different. The Wilkes Land anticyclone is now larger and has moved closer to the Ross Ice Shelf. It is evident that a larger portion of the East Antarctic moisture transport is being entrained around the anticyclone and that the ridge and trough have become a combined entity. The Ross Ice Shelf vortex has also diminished in longitudinal extent. The pattern shown for 1992 is nearly identical for the 4 year period from 1991 to 1994. Several authors have examined southern hemisphere blocking patterns [e.g., *Trenberth and Mo*, 1985; *Sinclair*, 1996] but have not discussed this area in detail. A previous study has considered the winter impact of similar ridging on much shorter timescales, with subsequent impact on the Amundsen Sea Low and development of katabatic surge events over the Ross Ice Shelf [*Bromwich et al.*, 1993a, see their Figure 13]. An impact on the Southern Ocean storm track was inferred, resulting in a greater number of and/or more intense synoptic scale cyclones entering the Amundsen Sea. From the current study it is apparent that interannual variability in the atmospheric circulation in this region has decreased with the onset of the blocking pattern. Both the SLP and the 500-hPa fields are remarkably consistent over the 4-year time period from 1991 to 1994, in contrast to variability seen in the 1980s.

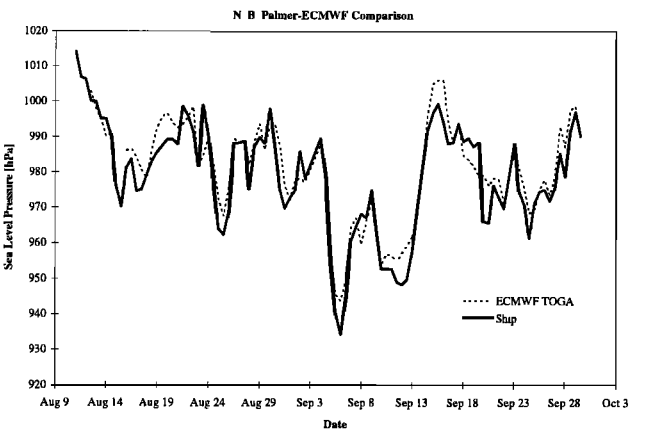

Figure 7. Mean sea level pressure from *Nathaniel B. Palmer* and interpolated from ECMWF WCRP/TOGA analysis for August and September 1993, in hectopascals.

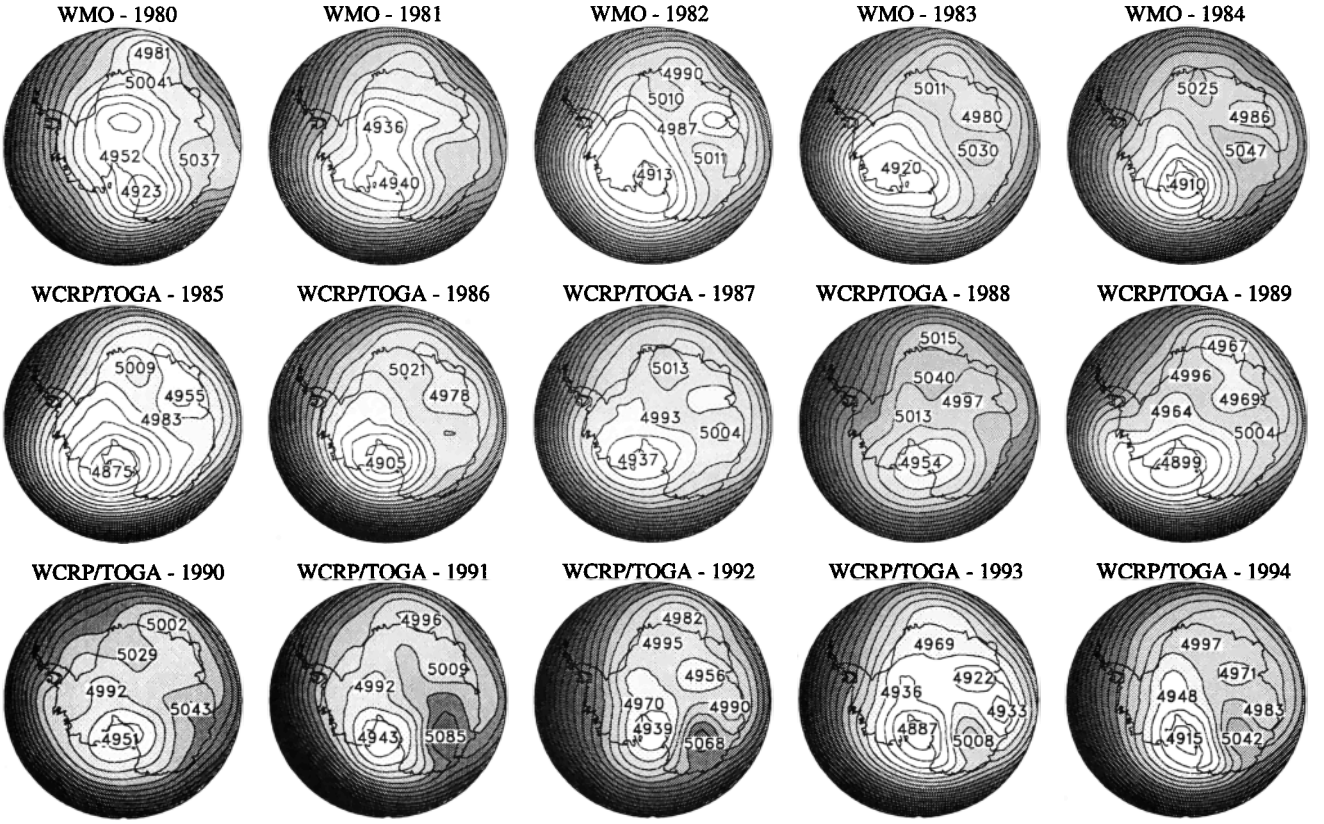

Figure 8. Annually-averaged 500-hPa geopotential height fields for 15 years, contoured every 20 geopotential meters.

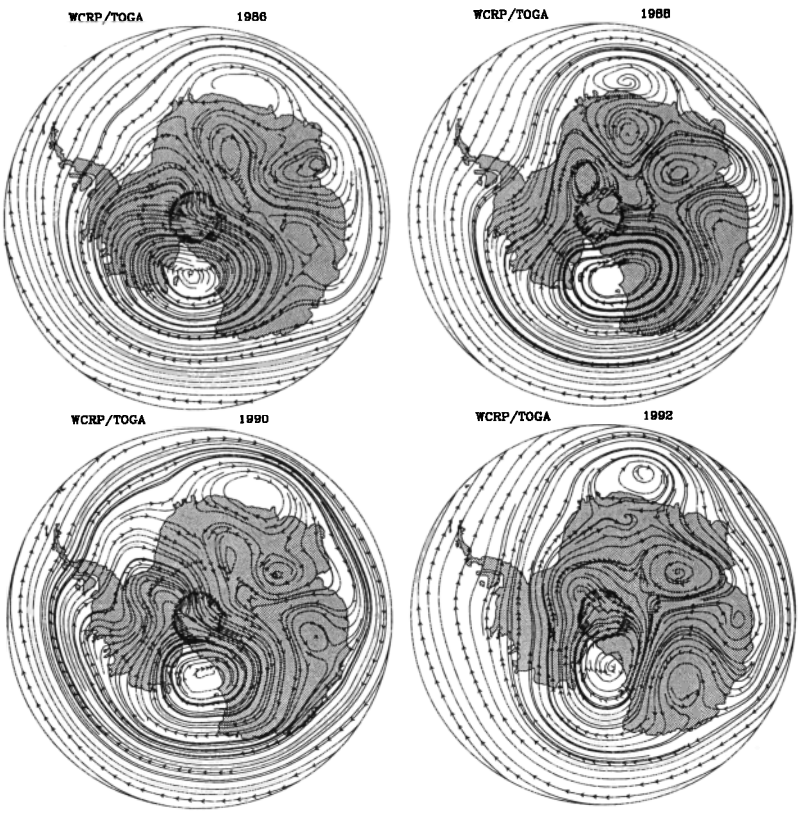

Figure 9. Streamline plots of annually averaged mean moisture transport at 500 hPa for 1986 (upper left), 1988 (upper right), 1990 (lower left), and 1992 (lower right).

Antarctic Precipitation from the NCEP/NCAR Reanalysis

As previously mentioned, a major obstacle to using operationally analyzed data for climatic study is the effect of alterations in the data assimilation system on the climatic ensemble of analyses. An alternative is the use of data sets recently produced by "reanalysis" projects [*Bengtsson and Shukla*, 1988; *Trenberth*, 1995; *Kalnay et al.*, 1996], in which the numerical analysis is performed in a consistent manner over the duration of the data set. Additionally, a larger array of analyzed and forecasted fields are produced than are operationally available. Here the monthly averaged precipitation fields from the NCEP/NCAR reanalysis project are assessed over the West Antarctic domain. Net precipitation interannual variability is dominated by the precipitation field, and evaporation/sublimation is discounted. In the NCEP/NCAR reanalysis, precipitation is classified as type "C", which designates fields that are strongly dependent on model physics. Unlike the moisture budget approach, which uses the analyzed fields constrained by observational data, the precipitation fields are forecasts and hence are vulnerable to the limitations associated with the forecast model, including model assumptions of the precipitation mechanisms.

Figure 10a shows the NCEP/NCAR reanalysis precipitation distribution for Antarctica averaged from monthly fields for 1982-1994. The field shows spurious wave patterns occurring near the south pole which are characterized by large maxima and appear to be related to the spectral noise of the model. Unlike the ECMWF precipitation fields examined by *Genthon and Braun* [1995], there are substantial differences between the NCEP/NCAR reanalysis spatial distribution depicted in Figure 10a and the long-term annual accumulation map synthesized from observation by *Giovinetto and Bentley* [1985]. In the area of interest in West Antarctica, Figure 10a shows maxima near 100°W encircling an area of elevated topography. The Giovinetto and Bentley map indicates an area of low accumulation over West Antarctica extending onto the Ross Ice Shelf; however, the observed gradients are substantially less, and the reanalysis values exceed observation by a factor of 10 for locations where Figure 10a depicts bull's-eyes along the eastern edge of the Ross Ice Shelf and the northern coast of West Antarctica. The line of precipitation extending from the west side of the Antarctic Peninsula to south pole, as well as the various splotches over the East Antarctic plateau region, are bogus and cannot be reconciled with observation using any plausible evaporation/sublimation field. The depicted splotches vary in magnitude with time but are geographically fixed. If the assumption is made that the NCEP/NCAR reanalysis precipitation field is more closely related to observation when averaged over a large area, then a temporal comparison may be useful. When the region defined in Figure 2 is examined, the time series shows a somewhat linear trend in annually averaged precipitation from 1982 to 1989, with an abrupt step increase in annual precipitation occurring in 1990. When the averaging sector is moved to include the maxima near 100°W, the time series, shown in Figure 10b, is found to be qualitatively similar to that depicted in Figure 3. Figure 10b shows a similarity between the SOI and moisture convergence from 1982 until 1990, with minima roughly corresponding to the 1982-1983 and 1987 ENSO warm events and a maximum corresponding to the 1988 cold event. After 1990, the two

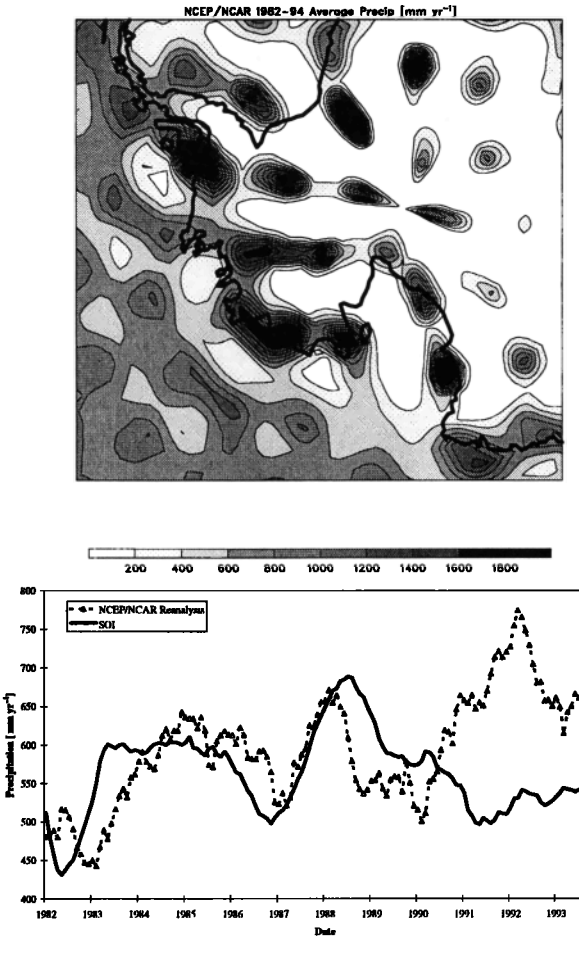

Figure 10. (a) Average areal distribution of precipitation from the NCEP/NCAR reanalysis for 1982-1994 over West Antarctica. (b) Annual running mean of NCEP/NCAR reanalysis precipitation for Antarctic region bounded by 90°W, 150°W, and 75°S, in millimeters per year, in comparison with the SOI.

curves diverge, with moisture convergence increasing dramatically as the SOI becomes negative over an extended period of time. The similarity with Figure 4 is only approximate, which is expected given the spatial discrepancies.

4. Discussion

The large variability in moisture convergence presented in this study implies a dramatic impact on global sea level. Interannual oscillations of more than 30% in Antarctic annual net precipitation shown here represent a global sea level variability range of ±1.2-1.5 mm yr^{-1} based on estimated continental ice accumulation excluding the oceanic ice shelves, which do not contribute to sea level changes [*Jacobs et al.*, 1992, see their Table 2].

There is uncertainty as to whether this figure is large in comparison with interannual variability in the global sea level. The eustatic rise is generally accepted to be of the order of 1-3 mm yr^{-1}, as derived from tide gauge measurements [*Gornitz et al.*, 1982; *Godfrey and Love*, 1992; *Gornitz*, 1993, 1995]. The tide gauge record, however, also indicates considerable year to year variability, typically of the order of

several centimeters [*Gornitz et al.*, 1982; *Gornitz*, 1993]. It is interesting to note that recent satellite-derived measurements contradict this result. Global sea level variability derived from 2 years of Geosat data [*Tapley et al.*, 1992] and the 2.5-year analysis of TOPEX/Poseidon data [*Nerem*, 1995] both indicate short-term eustatic change to be of the order of a few millimeters. It has been suggested that the tide gauge network is inadequate for the determination of sea level variability [e.g., *Gröger and Plag*, 1993], and this is consistent with the satellite result. If the satellite findings are accurate, the contribution determined here is large in relation to the present interannual global sea level variability. The large variability necessitates a long time series in order to evaluate the Antarctic contribution to the global sea level rise.

U.S. projects are currently planned for attaining ice cores in West Antarctica [*Bindschadler*, 1992]. The temporally varying ENSO signal should be resolved in strategically placed ice cores in West Antarctica. Inconclusive initial comparisons using individual ice cores have been performed using Siple Station (76°S, 84°W) and Dyer Plateau cores (71°S, 65°W) (L.G. and E.M. Thompson, personal communication, 1995); however, these sites are strongly affected by Weddell Sea conditions. This result is not surprising. For comparison with spatially averaged net precipitation from numerical analyses, an array of ice cores is required. This procedure was successfully used to study Greenland precipitation [*Bromwich et al.*, 1993b; *Bolzan and Strobel*, 1994].

The positioning of the Amundsen Sea Low is identified in this paper as a catalyst for the observed ENSO precipitation variability. It is interesting to note that this positioning is in some ways analogous to the northern hemisphere Aleutian Low, which moves southeastward of its mean position during ENSO events and increases the southerly flow over the Bering Sea [*Bjerknes*, 1969; *Niebauer and Day*, 1989]. Although not discussed, the Amundsen Sea Low has previously been depicted by *Schwerdtfeger* [1984, see his Figures 4.1.a and 4.1.b]. The annually averaged climatological low is the result of wintertime positioning in the Ross Sea and the summertime low pressure that forms to the west of the Antarctic Peninsula. The annually averaged low thus appears to be the dominance of one season over another. At present, it is thought that the positioning of the Amundsen Sea Low is the product of several factors, including the large-scale circulation, the South Pacific storm track, and mass transport resulting from the Antarctic katabatic wind flow. *King* [1994] has examined the highly interrelated climatic mechanisms in the Peninsula area, and notes the extreme climatic sensitivity of the region. The results presented here do not challenge this contention.

Acknowledgments. This research was sponsored by the National Aeronautics and Space Administration under grants NAGW-3677 to the second author and W-18795 to the third author. This is contribution 1008 of Byrd Polar Research Center.

References

Arpe, K., and H. Cattle, A comparison of surface stress and precipitation fields in short-range forecasts over the Antarctic region, *J. Geophys. Res.*, *98*, 13,035-13,044, 1993.

Bengtsson, L., and J. Shukla, Integration of space and in situ observations to study global change, *Bull. Am. Meteorol. Soc.*, *69*, 1130-1143, 1988.

Bindschadler, R.A. (Ed.), First annual West Antarctic Ice Sheet (WAIS) science workshop, *NASA Conf. Publ.*, *3222*, 58 pp., 1992.

Bjerknes, J., Atmospheric teleconnections from the equatorial Pacific, *Mon. Weather Rev.*, *97*, 162-172, 1969.

Bluestein, H.B., *Synoptic-Dynamic Meteorology in Midlatitudes*, Volume II, *Observations and Theory of Weather Systems*, pp. 79-80, Oxford Univ. Press, New York, 1993.

Bolzan, J.F., and M. Strobel, Accumulation rate variations around Summit, Greenland, *J. Glaciol.*, *40*, 56-66, 1994.

Bromwich, D.H., Snowfall in high southern latitudes, *Rev. Geophys.*, *26*, 149-168, 1988.

Bromwich, D.H., Estimates of Antarctic precipitation, *Nature*, *343*, 627-629, 1990.

Bromwich, D.H., and F.M. Robasky, Recent precipitation trends over the polar ice sheets, *Meteorol. Atmos. Phys.*, *51*, 259-274, 1993.

Bromwich, D.H., A.M. Carleton, and T.R. Parish, A review of precipitation-related aspects of West Antarctic meteorology, *NASA Conf. Publ.*, *3115*, vol. 2, 1-15, 1991.

Bromwich, D.H., J.F. Carrasco, Z. Liu, and R.-Y. Tzeng, Hemispheric atmospheric variations and oceanographic impacts associated with katabatic surges across the Ross Ice Shelf, Antarctica, *J. Geophys. Res.*, *98*, 13045-13062, 1993a.

Bromwich, D.H., F.M. Robasky, R.A. Keen, and J.F. Bolzan, Modeled variations of precipitation over the Greenland ice sheet, *J. Clim.*, *6*, 1253-1268, 1993b.

Bromwich, D.H., F.M. Robasky, R.I. Cullather, and M.L. Van Woert, The atmospheric hydrologic cycle over the Southern Ocean and Antarctica from operational numerical analyses, *Mon. Weather Rev.*, *123*, 3518-3538, 1995.

Budd, W.F., P.A. Reid, and L.J. Minty, Antarctic moisture flux and net accumulation from global atmospheric analyses, *Ann. Glaciol.*, *21*, 149-156, 1995.

Carleton, A.M., Sea ice-atmosphere signal of the Southern Oscillation in the Weddell Sea, Antarctica, *J. Clim.*, *1*, 379-388, 1988.

Carleton, A.M., Antarctic sea-ice relationships with indices of the atmospheric circulation of the Southern Hemisphere, *Clim. Dyn.*, *3*, 207-220, 1989.

Chen, B., S.R. Smith, and D.H. Bromwich, Evolution of the tropospheric split jet over the South Pacific Ocean during the 1986-1989 ENSO cycle, *Mon. Weather Rev.*, *124*, 1711-1731, 1996.

Chiu, L.S., Antarctic sea ice variations 1973-1980, in *Variations in the Global Water Budget*, edited by A. Street-Perrott, M. Beran, and R. Ratcliffe, pp. 301-311, D. Reidel, Norwell, Mass., 1983.

Dayton, P.K., Interdecadal variation in an Antarctic sponge and its predators from oceanographic climate shifts, *Science*, *245*, 1484-1486, 1989.

Escoffier, C., and C. Provost, Wind forcing over the southwest Atlantic: Comparisons between observations and ECMWF analyses, *Mon. Weather Rev.*, *123*, 1269-1287, 1995.

Genthon, C., and A. Braun, ECMWF analyses and predictions of the surface climate of Greenland and Antarctica, *J. Clim.*, *8*, 2324-2332, 1995.

Giovinetto, M.B., and C.R. Bentley, Surface balance in ice drainage systems of Antarctica, *Antarct. J. U.S.*, *20*(4), 6-13, 1985.

Giovinetto, M.B., D.H. Bromwich, and G. Wendler, Atmospheric net transport of water vapor and latent heat across 70°S, *J. Geophys. Res.*, *97*, 917-930, 1992.

Gloersen, P., Modulation of hemispheric sea-ice cover by ENSO events, *Nature*, *373*, 503-506, 1995.

Godfrey, J.S., and G. Love, Assessment of sea level rise, specific to the South Asian and Australian situations, in *Sea Level Changes: Determination and Effects*, *Geophys. Monogr. Ser.*, vol. 69, edited by P.L. Woodworth et al., pp. 87-94, AGU, Washington, D.C., 1992.

Gornitz, V., Mean sea level changes in the recent past, in *Climate and Sea Level Change*, edited by R.A. Warrick, E.M. Barrow, and T.M.L. Wigley, pp. 25-44, Cambridge Univ. Press, New York, 1993.

Gornitz, V., Monitoring sea level changes, *Clim. Change*, *31*, 515-544, 1995.

Gornitz, V., S. Lebedeff, and J. Hansen, Global sea level trend in the past century, *Science*, *215*, 1611-1614, 1982.

Gröger, M., and H.-P. Plag, Estimations of a global sea level trend:

Limitations from the structure of the PSMSL global sea level data set, *Global Planet. Change*, *8*, 161-179, 1993.

Harangozo, S.A., The impact of the semi-annual cycle on South Pacific sea ice extent in two contrasting years, in *Fourth Conference on Polar Meteorology and Oceanography*, pp. 162-167, Am. Meteorol. Soc., Boston, Mass., 1995.

Jacobs, S.S., Is the Antarctic ice sheet growing?, *Nature*, *360*, 29-33, 1992.

Jacobs, S.S., H.H. Helmer, C.S.M. Doake, A. Jenkins, and R.M. Frolich, Melting of ice shelves and the mass balance of Antarctica, *J. Glaciol.*, *38*, 375-387, 1992.

Jeffries, M.O., R/V Nathaniel B. Palmer cruise NBP93-5: Sea-ice physics and biology in the Bellingshausen and Amundsen Seas, August and September 1993, *Antarct. J. U.S.*, *29*(1), 7-8, 1994.

Kalnay, E., et al., The NCEP/NCAR 40-year reanalysis project, *Bull. Am. Meteorol. Soc.*, *77*, 437-471 plus CD-ROM, 1996.

Karoly, D.J., Southern Hemisphere circulation features asociated with El Niño-Southern Oscillation events, *J. Clim.*, *2*, 1239-1252, 1989.

King, J.C., Recent climate variability in the vicinity of the Antarctic Peninsula, *Int. J. Climatol.*, *14*, 357-369, 1994.

Kitoh, A., Tropical influence on the South Pacific double jet variability, *Proc. NIPR Symp. Polar Meteorol. Glaciol.*, *8*, 34-45, 1994.

Lettau, B., The transport of moisture into the antarctic interior, *Tellus*, *21*, 331-340, 1969.

National Research Council, *El Niño and the Southern Oscillation: A Scientific Plan*, 63 pp., Nat. Acad. Press, Washington, D.C., 1983.

Nerem, R.S., Measuring global mean sea level variations using TOPEX/Poseidon altimeter data, *J. Geophys. Res.*, *100*, 25,135-25,151, 1995.

Newell, R.E., L.S. Chiu, W. Ebisuzaki, A.R. Navato, and H.B. Selkirk, The oceans and ocean currents: Their influence on climate, in *International Conference on Climate and Offshore Energy Resources*, pp. 59-112, Am. Meteorol. Soc., Boston, Mass., 1981.

Niebauer, H.J., and R.H. Day, Causes of interannual variability in the sea ice cover of the eastern Bering Sea, *GeoJournal*, *18*(1), 45-59, 1989.

Oerlemans, J., A projection of future sea level, *Clim. Change*, *15*, 151-174, 1989.

Pittock, A.B., On the reality, stability, and usefulness of southern hemisphere teleconnections, *Aust. Meteorol. Mag.*, *32*, 75-82, 1984.

Priddle, J., J.P. Croxall, I. Everson, R.B. Heywood, E.J. Murphy, P.A. Prince, and C.B. Sear, Large-scale fluctuations in distribution and abundance of krill: a discussion of possible causes, in *Antarctic Ocean and Resources Variability*, edited by S. Dietrich, Springer-Verlag, New York, pp. 169-182, 1988.

Savage, M.L., C.R. Stearns, and G.A. Weidner, The Southern Oscillation signal in Antarctica, in *Second Conference on Polar Meteorology and Oceanography*, pp. 141-144, Am. Meteorol. Soc., Boston, Mass., 1988.

Schwerdtfeger, W., *Weather and Climate of the Antarctic*, *Dev. in Atmos. Sci. Ser.*, vol. 15, 261 pp., Elsevier, New York, 1984.

Simmonds, I., and T.H. Jacka, Relationships between interannual variability of Antarctic sea ice and the Southern Oscillation, *J. Clim.*, *8*, 637-647, 1995.

Sinclair, M.R., A climatology of anticyclones and blocking in the Southern Hemisphere, *Mon. Weather Rev.*, *124*, 245-263, 1996.

Smith, S.R., and D.H. Bromwich, Behavior of the tropospheric split jet stream over the South Pacific Ocean during the 1986-1990 ENSO cycle, in *Sixth Conference on Climate Variations*, pp. 278-282,, Am. Meteorol. Soc., Boston, Mass., 1994.

Smith, S.R., and C.R. Stearns, Antarctic pressure and temperature anomalies surrounding the minimum in the Southern Oscillation Index, *J. Geophys. Res.*, *98*, 13,071-13,083, 1993a.

Smith, S.R., and C.R. Stearns, Antarctic climate anomalies surrounding the minimum in the Southern Oscillation Index, in *Antarctic Meteorology and Climatology: Studies Based on Automatic Weather Stations*, *Antarct. Res. Ser.*, vol. 61, edited by D.H. Bromwich and C.R. Stearns, pp. 149-174, AGU, Washington, D.C., 1993b.

Smith, S.R., D.H. Bromwich, and B. Chen, Split jet evolution over the South Pacific Ocean during the 1986-1989 ENSO cycle, in *Fourth Conference on Polar Meteorology and Oceanography*, pp. 246-251, Am. Meteorol. Soc., Boston, Mass., 1995.

Stearns, C.R., L.M. Keller, G.A. Weidner, and M. Sievers, Monthly mean climatic data for Antarctic automatic weather stations, in *Antarctic Meteorology and Climatology: Studies Based on Automatic Weather Stations*, *Antarct. Res. Ser.*, vol. 61, edited by D.H. Bromwich and C.R. Stearns, pp. 1-21, AGU, Washington, D.C., 1993.

Swarztrauber, P.N., The direct solution of the discrete poisson equation on the surface of a sphere, *J. Comput. Phys.*, *15*, 46-54, 1974.

Tapley, B.D., C.K. Shum, J.C. Ries, R. Suter, and B.E. Schutz, Monitoring of changes in global mean sea level using Geosat altimeter, in *Sea Level Changes, Determination and Effects*, *Geophys. Monogr. Ser.*, vol. 69, edited by P.L. Woodworth et al., pp. 167-180, AGU, Washington, D.C., 1992.

Testa, J.W., G. Oehlert, D.G. Ainley, J.L. Bengtson, D.B. Siniff, R.M. Laws, and D. Rounsevell, Temporal variability in Antarctic marine ecosystems: Periodic fluctuations in the phocid seals, *Can. J. Fish. Aquat. Sci.*, *48*, 631-639, 1991.

Trenberth, K.E., General characteristics of El Niño-Southern Oscillation, in *Teleconnections Linking Worldwide Climate Anomalies: Scientific Basis and Societal Impact*, edited by M.H. Glantz, R.W. Katz, and N. Nicholls, pp. 13-42, Cambridge Univ. Press, New York, 1991a.

Trenberth, K.E., Climate diagnostics from global analyses: Conservation of mass in ECMWF analyses. *J. Clim.*, *4*, 707-722, 1991b.

Trenberth, K.E., Global analyses from ECMWF and atlas of 1000 to 10 mb circulation statistics, *NCAR Tech. Note, NCAR/TN-373+STR*, 191 pp. plus 24 fiche, Natl. Cent. for Atmos. Res., Boulder, Colo., 1992.

Trenberth, K.E., Atmospheric circulation climate changes, *Clim. Change*, *31*, 427-453, 1995.

Trenberth, K.E., and C.J. Guillemot, Evaluation of the global atmospheric moisture budget as seen from analyses, *J. Clim.*, *8*, 2255-2272, 1995.

Trenberth, K.E., and T.J. Hoar, The 1990-1995 El Niño-Southern Oscillation event: Longest on record, *Geophys. Res. Lett.*, *23*, 57-60, 1996.

Trenberth, K.E., and K.C. Mo, Blocking in the Southern Hemisphere, *Mon. Weather Rev.*, *113*, 3-21, 1985.

van Loon, H., and D.J. Shea, The Southern Oscillation, VI, Anomalies of sea level pressure on the Southern Hemisphere and of Pacific sea surface temperature during the development of a warm event, *Mon. Weather Rev.*, *115*, 370-379, 1987.

Xie, S., C. Bao, Z. Xue, L. Zhang, and C. Hao, Interaction between Antarctic sea ice and ENSO events, *Proc. NIPR Symp. Polar Meteorol. Glaciol.*, *8*, 95-110, 1994.

Yamazaki, K., Moisture budget in the Antarctic atmosphere, *Proc. NIPR Symp. Polar Meteorol. Glaciol.*, *6*, 36-45, 1992.

D. H. Bromwich and R. I. Cullather, Polar Meteorology Group, Byrd Polar Research Center, The Ohio State University, Columbus, OH 43210-1002.

M. L. Van Woert, Office of Naval Research, Arlington, VA 22217-0001.

(Received August 18, 1995; revised April 22, 1996; accepted May 30, 1996.)